Photopolymerization of Maleimide Perfluoropolyalkylethers without a Photoinitiator

Céline Bonneaud,[1] **Julia M. Burgess**,[2] **Roberta Bongiovanni**,[3] **Christine Joly-Duhamel**,[1] **Chadron M. Friesen**[2]

[1]Ingénierie et Architectures Macromoléculaires, Institut Charles Gerhardt, Ecole Nationale Supérieure de Chimie de Montpellier (UMR5253-CNRS), 8, rue de l'Ecole Normale, 34296, Montpellier Cedex 5, France
[2]Department of Chemistry, Trinity Western University, 7600 Glover Road, Langley, British Columbia V2Y 1Y1, Canada
[3]Department of Applied Science and Technology, Politecnico di Torino, c. Duca degli Abruzzi 24, 10129, Torino, Italy
Correspondence to: C. M. Friesen (E-mail: chad.friesen@twu.ca) and C. Joly-Duhamel (E-mail: christine.joly-duhamel@enscm.fr)

Received 14 November 2018; accepted 10 December 2018
DOI: 10.1002/pola.29311

ABSTRACT: Perfluoropolyalkylethers derived from hexafluoropropylene oxide were functionalized with maleimide groups. Irradiated by UV-light, the new maleimide macromonomers demonstrated very fast polymerization kinetics with a curing time as fast as 8 s. The effect on photopolymerization of different features such as the molecular weight of the fluorinated chain and the chain length of the hydrogenated spacer were studied, as well as the influence of the type of photoinitiator and the presence of air. Thermal and surface properties of the UV-cured polymers were examined and were typical to fluoropolymers in view of water–oil repellent coatings. © 2018 Wiley Periodicals, Inc. J. Polym. Sci., Part A: Polym. Chem. **2018**

KEYWORDS: perfluoropolyalkylethers; photopolymerization; maleimides; omniphobicity

INTRODUCTION Photopolymerization is a green process: it occurs rapidly without a solvent and at room temperature.[1] Commonly, photopolymerized systems are constituted of (meth)acrylates or thiol-enes.[2–5] Maleimides are alternative systems which polymerize almost as fast as acrylates but do not require a photoinitiator. Indeed, maleimides can initiate the polymerization on their own as displayed in Scheme 1. The mechanism of initiation was found to be an electron transfer, which provides a radical anion. It was supported by Fourier Transform-Electron Paramagnetic Resonance and by flash laser photolysis.[6,7] Thus, maleimides can homopolymerize without a photoinitiator[8] as the presence of photoinitiator can lead to their leaching or their hard removal if used in excess. Moreover, maleimides can serve as photoinitiators for different types of unsaturated resins (acrylate, vinyl ether, and epoxy).[9,10]

Various types of maleimides were tested under UV-light such as poly(propylene glycol)-maleimides[8] or silicon-maleimides[11,12] and demonstrated the high ability of polymerization of the maleimides even in presence of long chains.

Maleimides have been found to be very useful in variety of polymer systems from "click" chemistry, self-healing polymers to thermoset polymers with high temperature stability.[13] However, the body of work only demonstrated a minimal amount of fluorine content attached to maleimides, ranging from single fluorines, $-CF_3$ to C_6F_{13} moieties. Barrales-Rienda et al.[14] reported in 1977 the first synthesis of fluorine-containing maleimides and their thermal polymerization using 2,2′-azobisisobutyronitrile (AIBN).[15] Much later, Mokhtar et al.[16] synthesized another maleimide, 4-(4-trifluoromethyl)phenoxy *N*-phenyl-maleimide which was also polymerized using AIBN. Maleimides containing pentafluoro and trifluoro groups on aromatics were copolymerized with vinyl ethers by Hendlinger et al.[17] whereas Jain et al.[18] copolymerized *N*-(4-fluoro phenyl) maleimide with methyl methacrylate. Daukiya et al.[19] showed the use of *N*-(3,4-trifluoro phenyl) maleimide with highly non-reactive graphene. Fluorinated oligomers with maleimides were first reported by Beaune et al. with C_6F_{13} chains.[20] Boutevin et al.[21] also demonstrated that maleimide-containing C_6F_{13} moieties can also be grafted onto high density polyethylene. Few examples of fluorinated telechelic bis(maleimides) can be found having as spacers a perfluoroalkyl chain[22] or fluorinated aromatics[23] or even difluoromaleimides as telechelic end groups.[24] Lastly, maleimides have been found to be useful in medical applications for radiolabeling. For example, *N*-(*p*-[18F]fluorophenyl)maleimide was used to label monoclonal antibodies.[25] Various maleimide-based compounds were exploited as reagents for protein, peptide and lipids labeling with thiol functions[26–28] and thus used in positron emission tomography imaging.[29,30]

Additional supporting information may be found in the online version of this article.

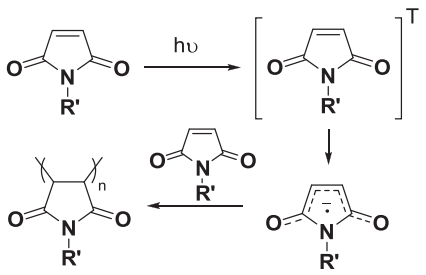

SCHEME 1 Homopolymerization of maleimides by radical mechanism.

In this study, we synthesized new maleimides characterized by perfluoropolyalkylether (PFPAE) chains, based on hexafluoropropyleneoxide (HFPO) unit —$CF(CF_3)CF_2O$—. The synthesized monomers have a general structure maleimide-R_h-R_f where R_f = $CF_3CF_2CF_2O(CF(CF_3)CF_2O)_n$ $CF(CF_3)$— with n = 5.5 and 10 and R_h = —$(CH_2)_m(CO)OCH_2$— with m = 3, 5, 10. The new monomers were photopolymerized to obtain new polymeric materials with promising performances due to the long fluorinated PFPAES chains. Notably, PFPAE polymers which contain ether units such as —(CF_2O)—, —(CF_2CF_2O)—, —$(CF_2CF_2CF_2O)$—, and —$(CF(CF_3)CF_2O)$— are known to demonstrate excellent chemical and thermal inertness with low surface energy. They are not crystalline and are stable from −100 and 400 °C in the liquid state.[31] Moreover, they are attractive for use since they are non-toxic fluoropolymers in comparison to some perfluoroalkyl chains and therefore can be employed in biomedical applications.[32–34]

The influences of the molecular weight of the fluorinated chain, the hydrogenated spacer length as well as the presence of air and photoinitiator on cure time and thermal degradation were studied.

EXPERIMENTAL

Materials

Glacial acetic acid, 11-maleimidoundecanoïc acid, 6-amin ocaproic acid, 4-aminobutyric acid, maleic anhydride, thionyl chloride, triethylamine, dicyclohexylcarbodiimide, 4-dimethyl aminopyridine, 2-hydroxy-2-methylpropiophenone (Darocur 1173), diphenyl(2,4,6-trimethylbenzoyl)phosphine oxide (TPO), phenylbis(2,4,6-trimethylbenzoyl)phosphine oxide (BAPO), dich loromethane, hexadecane, and deuterated solvents (DMSO-*d6*, $CDCl_3$ and C_6D_6) were purchased from Sigma Aldrich and used as received except if stated below. 1,1,1,3,3-pentafluorobutane was purchased from Alfa Aesar. The 1250 g/mol oligo (HFPO) methylene alcohol was prepared from Krytox® acyl fluoride. The 1250 g/mol Krytox® acyl fluoride and 2000 g/mol Krytox® methylene alcohol were kindly provided by the Chemours Company. Triethylamine, hexadecane, and dichloromethane were dried for 48 h over preconditioned 3 Å molecular sieves (20% w/v). Thionyl chloride was previously distilled before use.

Methods

Photopolymerization by Fourier-Transform–Real Time Infrared Spectroscopy

Real-time Infrared Spectroscopy and photopolymerization kinetics were performed on a Thermo Scientific Nicolet 6700 FTIR apparatus by using OMNIC software. A mercury lamp (OmniCure S2000) was used as UV-light source and OmniCure R2000 Radiometer was used to control the light output. A radiometer from Solatell provided a real light intensity on the sample of 10 mW cm^{-2}. A polypropylene film (6 μm) was used as air protector. The sample was irradiated during 300 s at least. Four repeats were made for each experiment. No photoinitiator was added except if specified. The conversion rate calculations were made by following the disappearance of the band at 826 cm^{-1} corresponding to the maleimide. They were calculated using the univariate method ($\tau = (1 - (A/A_0)) \times 100$). The peak deconvolution method was used to confirm the quantitative conversion. When required, an UV production curing unit Fusion UV F300S equipped with a microwave lamp (linear power output of 120 W cm^{-1}) was utilized. The sample was placed on a LC6B Bench top conveyor and passed repeatedly under the UV lamp at a speed of travel belt of 1 m min^{-1}.

Gas Chromatography (GC) Mass Spectrometry (MS)

An Agilent Technologies 6890N GC was coupled with an Agilent Technologies 7638B series injector and Agilent Technologies 5975B inert mass spectrometer (MSD) was employed with electron impact as the mode of ionization. The GC was equipped with a Zebron ZB-5 ms column, 30 m × 0.18 mm id, 0.18 μm df. The detector and the injector temperatures were 200 and 280 °C, respectively. The temperature program started from 50 °C with a 2 min hold, then the heating rate was 25 °C min^{-1} until reaching 250 °C and holding at 250 °C for 2 min. The total pressure 108 kPa, total flow was 25.9 mL min^{-1}, column flow 0.74 mL min^{-1}, purge flow 3 mL min^{-1}, linear velocity 38 2 cm s^{-1}, and a split injection of 30:1. The sample was previously diluted in methoxyperfluorobutane (3M's Novec™ HFE-7100) in a GC vial.

Nuclear Magnetic Resonance (NMR) spectroscopy

NMR spectra were recorded on a Bruker AVANCE III 400 MHz spectrometer instruments using TopSpin 3.5 operating at 400.13 (^{1}H), 376.46 (^{19}F), and 100.62 (^{13}C) MHz at room temperature except if specified. $CDCl_3$ and C_6D_6 capillaries were used as internal references. The letters s, d, t, q, quint, sext, and spt stand for singlet, doublet, triplet, quartet, quintuplet, sextet and septuplet, respectively.

Matrix Assisted Laser Desorption Ionization Time-of-Flight Mass Spectrometry (MALDI-TOF-MS)

The homologue distributions of the products were determined with a Bruker Autoflex™ *MALDI-TOF:* spectrometer equipped with a 1 kHz smartbeam-II laser and reflector in positive ionization. For sample preparation, a one drop sample of poly(HFPO) was added to a 1 mL solution of 50:50 1% LiCl in MeOH and 2% perfluorocinnamic acid dissolved in 50:50 MeOH:Methoxynonafluorobutane (3 M HFE-7100). A 1 μL

solution was then pipetted on to a ground steel plate, dried, and irradiated for a minimum of 5000 shots.

Thermogravimetric Analyses (TGA)

The degradation temperatures were determined with a NETZSCH TG209F1 at a heating rate of 20 or 10 °C min^{-1}. Approximately 10 mg of the sample was placed in an alumina crucible and heated from room temperature to 600 °C under inert atmosphere or air (40 mL min^{-1}). To analyze the evolved gases, the instrument is coupled with a FTIR PERSEUS Bruker heated at 200 °C and the obtained spectra are given between 4000 and 600 cm^{-1}.

Differential Scanning Calorimetry (DSC)

The glass transition temperatures were determined with a NETZSCH DSC200F3 calorimeter. Constant calibration was performed using indium, *n*-octadecane, and *n*-octane standards. Ten to fifteen milligrams were placed in pierced aluminum pans and the thermal properties were recorded between −150 and 100 °C at 20 °C min^{-1}. Nitrogen was used as the purge gas.

Contact Angle Measurements

The hydrophobicity and oleophobicity were determined; thanks to a contact angle system OCA20 coupled with a CCD-camera from DataPhysics Instrument using the software SCA20 4.1. The measurements were made in air at room temperature by the sessile drop technique with deionized water or previously dried hexadecane. Three repeats were made on three different samples previously spin-coated (1 min–2000 rpm) on glass slides; thanks to Spincoat G3-8 from Specialty Coating Systems and irradiated thanks to a UV bench conveyor. Their difference in the average value was not more than 3°.

Syntheses

Synthesis of 4-Maleimidobutyric Acid and 6-Maleimidohexanoic Acid (1a-b)

To a solution of maleic anhydride (2 g) in glacial acetic acid (15 mL), the corresponding amino acid was added (1 eq). The mixture was heated to reflux during 3 h. The solvent AcOH was evaporated via rotary evaporation by using toluene as azeotropic cosolvent. The crude material was extracted by using D.I. water (pH ~ 4) and EtOAc. The aqueous phase was washed two times with EtOAc. The organic phases were combined, dried with $MgSO_4$ and concentrated under vacuum to afford an orange oil. After drying in vacuum oven, the orange solids were washed with iced D.I. water (pH ~ 4) and dried in vacuum oven (70 °C) overnight to provide a whitish powder.

4-maleimidobutyric acid **1a** (yield = 27%): ^{1}H NMR (400 MHz, $CDCl_3$, δ): 1.92 (quint, $^3J_{H\text{-}H}$ = 7.1 Hz, —C**H$_2$**—, 2H), 2.35 (t, $^3J_{H\text{-}H}$ = 7.3 Hz, —C**H$_2$**COOH, 2H), 3.52 (t, $^3J_{H\text{-}H}$ = 6.9 Hz, —NC**H$_2$**—, 2H), 6.70 (s, —C**H**=C**H**—, 2H) ^{13}C NMR (101 MHz, $CDCl_3$, δ): 23.7 (—**C**H$_2$—), 31.1 (—**C**H$_2$COOH), 37.1 (—N**C**H$_2$—), 134.3 (—**C**H=**C**H—), 170.9 (— (**C**O) —CH=CH—(**C**O)—, 177.0 (—**C**OOH).

6-maleimidohexanoïc acid **1b** (yield = 35%): ^{1}H NMR (400 MHz, $CDCl_3$, δ): 1.3–1.37 (m, —C**H$_2$**—, 2H), 1.56–1.70 (m, —C**H$_2$**—, 4H), 2.35 (t, $^3J_{H\text{-}H}$ = 7.6 Hz, —C**H$_2$**COOH, 2H), 3.52 (t, $^3J_{H\text{-}H}$ = 7.3 Hz, —NC**H$_2$**—, 2H), 6.70 (s, —C**H**=C**H**—, 2H), 10.97 (s, —COO**H**, 1H) ^{13}C NMR (101 MHz, $CDCl_3$, δ): δ = 24.1 (—**C**H$_2$CH$_2$COOH—), 26.1 (—NCH$_2$CH$_2$**C**H$_2$—), 28.2 (—NCH$_2$**C**H$_2$—), 33.8 (—**C**H$_2$COOH—), 37.6 (—N**C**H$_2$—, 1C), 134.1 (—**C**H=**C**H—), 170.9 (— (**C**O)—CH=CH—(**C**O)—), 179.7 (—CH$_2$**C**OOH).

Synthesis of the Acid Chlorides (2b-c)

To a solution of the corresponding maleimido acid in dry DCM, 1.5 eq of triethylamine was added with 2 eq of thionyl chloride. The solution was heated at 50 °C for 3 h. The volatile compounds were removed under reduced pressure. The products were recovered quantitatively (yield >99%) as orange-brown solids.

6-maleimidohexanoyl chloride **2b** (yield>99%): ^{1}H NMR (400 MHz, $CDCl_3$, δ): 1.26 (m, —C**H$_2$**CH$_2$CH$_2$COCl—, 2H), 1.52 (quint, —C**H$_2$**CH$_2$COCl, 2H), 1.64 (quint, —NCH$_2$C**H$_2$**—, 2H), 2.82 (t, $^3J_{H\text{-}H}$ = 7.6 Hz, —C**H$_2$**COOH, 2H), 3.42 (t, $^3J_{H\text{-}H}$ = 7.33 Hz, —NC**H$_2$**—, 2H), 6.63 (s, —C**H**=C**H**—, 2H). ^{13}C NMR (101 MHz, $CDCl_3$, δ): 24.1 (—**C**H$_2$CH$_2$COOH—), 26.1 (—NCH$_2$CH$_2$**C**H$_2$—), 28.2 (—NCH$_2$**C**H$_2$—), 33.8 (—**C**H$_2$COOH—), 37.6 (—N**C**H$_2$—), 134.1 (—**C**H=**C**H—), 170.9 (—(CO)—C**H**=C**H**—(CO)—), 179.7 (—CH$_2$**C**OOCl).

11-maleimidoundecanoyl chloride **2c** (yield >99%): ^{1}H NMR (400 MHz, C_6D_6, δ): 1.47–1.51 (m, N—CH$_2$CH$_2$(C**H$_2$**)$_6$CH$_2$CH$_2$(CO)—, 12H), 1.76 (quint, N—CH$_2$C**H$_2$**(CH$_2$)$_6$—, $^3J_{H\text{-}H}$ = 6.6 Hz, 2H), 1.90 (quint, Cl(CO)—CH$_2$C**H$_2$**(CH$_2$)$_6$—, 2H), 3.12 (t, Cl(CO)C**H$_2$**—, $^3J_{H\text{-}H}$ = 7.2 Hz, 2H), 3.67 (t, —N—C**H$_2$**—, $^3J_{H\text{-}H}$ = 7.2 Hz, 2H), 6.90 (s, —C**H**=C**H**—, 2H). ^{13}C NMR (101 MHz, C_6D_6, δ): 24.8 (—NCH$_2$C**H$_2$**—), 28.1 (—**C**H$_2$CH$_2$COOH—), 29.2 (—CH$_2$CH$_2$(**C**H$_2$)$_6$CH$_2$CH$_2$(CO)—, 33.9 (—N**C**H$_2$—), 37.5 (—**C**H$_2$COOH—), 134.0 (—**C**H=**C**H—), 172.0 (—(**C**O)—CH=CH—(**C**O)—), 179.9 (—CH$_2$**C**OOCl).

Syntheses of Maleimide Poly(HFPO) M_w *~ 1250 g/mol*

To a mixture of oligo(HFPO) methylene alcohol and dry triethylamine (1.5 eq) in dry dichloromethane (DCM), a solution of the corresponding maleimido acid chloride (1 eq) in dry DCM was added dropwise. The mixture was then heated under reflux during 1 h. The volatiles were then removed under reduced pressure. The product was diluted in 1,1,1,3,3-pentafluorobutane and washed three times with Deionized (D.I.) water. After the removal of 1,1,1,3,3-pentafluorobutane, the product was filtrated through a 1.2 µm filter frit before photopolymerization.

M1 C5 **3b** (yield = 91%): ^{1}H NMR (400 MHz, C_6D_6, δ): 1.46 (quint, $^3J_{H\text{-}H}$ = 7.4 Hz, —N(CH$_2$)$_2$C**H$_2$**(CH$_2$)$_2$C(O)O—, 2H), 1.72 (quint, $^3J_{H\text{-}H}$ = 7.4 Hz, —NCH$_2$C**H$_2$**—, 2H), 1.81 (quint, $^3J_{H\text{-}H}$ = 7.38 Hz, N(CH$_2$)$_3$C**H$_2$**CH$_2$C(O)O—, 2H), 2.50 (t, $^3J_{H\text{-}H}$ = 7.4 Hz, —C**H$_2$**CO—, 2H), 3.61 (t, $^3J_{H\text{-}H}$ = 7.4 Hz, —NC**H$_2$**—, 2H), 4.79 (dd, $^2J_{H\text{-}H}$ = 30.3 Hz, –, $^3J_{H\text{-}F}$ = 12.9 Hz, —CF(CF$_3$)C**H$_2$**O—, 1H), 4.83 (dd, $^2J_{H\text{-}H}$ = 30.3 Hz, –, $^3J_{H\text{-}F}$ = 12.9 Hz, —CF(CF$_3$)C**H$_2$**O—, 1H), 6.90 (s, —C**H**=C**H**—, 2H) ^{13}C NMR (101 MHz, C_6D_6, δ): 23.7 (—C(O)CH$_2$C**H$_2$**—), 25.7 (—C(O)CH$_2$CH$_2$C**H$_2$**—), 27.9 (—NCH$_2$C**H$_2$**—), 32.7 (—C(O)C**H$_2$**), 36.8 (—NC**H$_2$**—), 59.0 (d, $^2J_{C\text{-}F}$ = 32.7 Hz, —CF(CF$_3$)C**H$_2$**O—), 133.6 (—C**H**=C**H**—),

170.0 (— (**C**O)—CH═CH—(**C**O)—), 170.6 (—O**C**(O) —) ^{19}F NMR (376 MHz, C_6D_6, δ): = —134.6 $R_fC\mathbf{F_2}(CF_3)CH_2O(CO)R_h$, GC–MS, 70 eV, *m/z*: 41.1 (13), 54.05 (10), 55.1 (24), 68.05 (12), 69.05 (65), 82.05 (18), 83.1 (13), 97.1 (31), 98.05 (26), 110.05 (100), 111.05 (23), 112.1 (12), 147 (14), 150.05 (13), 169 (45), 193.05 (22), 194.05 (54), FTIR (ATR) ν_{max} (cm^{-1}): 827.5–980.3–1119.0–1227.7–1709.8.

M1 C10 **3c** (yield = 95%): ^{1}H NMR (400 MHz, C_6D_6, δ): 1.45 m, —N$(CH_2)_2(C\mathbf{H_2})_6CH_2$—, 12H), 1.71 (quint, $^3J_{H\text{-}H}$ = 7.2 Hz, —NC$H_2C\mathbf{H_2}$—, 2H), 1.78 (quint, $^3J_{H\text{-}H}$ = 7.2 Hz, N$(CH_2)_8C\mathbf{H_2}CH_2C(O)O$—, 2H), 2.48 (t, $^3J_{H\text{-}H}$ = 7.2 Hz, —$CH_2C\mathbf{H_2}C(O)O$—, 2H), 3.61 (t, $^3J_{H\text{-}H}$ = 7.2 Hz, —NC$\mathbf{H_2}$—, 2H), 4.76 (dd, $^2J_{H\text{-}H}$ = 30.3 Hz, $^3J_{H\text{-}F}$ = 12.9 Hz, —$CF(CF_3)C\mathbf{H_2}O$—, 1H), 4.79 (dd, $^2J_{H\text{-}H}$ = 30.3 Hz, $^3J_{H\text{-}F}$ = 12.9 Hz, —$CF(CF_3)C\mathbf{H_2}O$—, 1H), 6.69 (s, —C**H**═C**H**—, 2H). ^{13}C NMR (101 MHz, C_6D_6, δ): 24.5 (—$\mathbf{C}H_2CH_2COO$—), 26.7 (—$NCH_2\mathbf{C}H_2$—), 28.5–29.2 (—$N(CH_2)_2(\mathbf{C}H_2)_6CH_2$—), 29.36 (—$CH_2\mathbf{C}H_2COO$—), 29.44 (—N**C**$H_2$—), 59.1 (d, $^2J_{C\text{-}F}$ = 32.7 Hz, —$CF(CF_3)\mathbf{C}H_2O$—), 133.5 (—**C**H═**C**H—), 170.0 0 (—(**C**O)—CH═CH—(**C**O)—), 170.6 (s, —O**C**(O)—). ^{19}F NMR (376 MHz, C_6D_6, δ): −134.4 $R_fC\mathbf{F_2}(CF_3)CH_2O(CO)R_h$ GC–MS, 70 eV, *m/z*: 41.1 (24), 55.1 (53), 69.05 (82), 81,1 (27), 82.05 (28), 83.1 (40), 97,1 (24), 98.05 (34), 100.05 (18), 110.05 (100), 111.05 (45), 119.05 (13), 147.1 (28), 149.15 (31), 150.05 (14), 169 (45), 191.15 (13), 263.15 (43), 264.15 (89), FTIR (ATR) ν_{max} (cm^{-1}): 827.4–980.7–1119.8–1228.4–1708.8.

Syntheses of Maleimide Poly(HFPO) M_w *~ 2000 g/mol*

To a solution of oligo(HFPO) methylene alcohol (M_w = 2000 g/mol, 2 g, 1 mmol), the corresponding maleimide (2 eq) and DMAP (0.1 eq) in 1,1,1,3,3-pentafluorobutane (15 mL), 2.2 eq of DCC in DCM (10 mL) were added dropwise at 0 °C during 30 min. After 5 min of reaction, the ice bath was removed. The conversion of the reaction was followed by ^{19}F NMR. After 30 min, the reaction was stopped. The reaction mixture was filtrated and concentrated under vacuum. Flash column chromatography by solid deposit with silica was performed (15:85 EtOAc:Pentane). The solvents were removed under vacuum to afford white blurry oils.

M2 C3 **4a** (yield = 69%): ^{1}H NMR (400 MHz, C_6D_6, δ): 1.81 (br, —$NCH_2C\mathbf{H_2}CH_2$—, 2H), 2.34 (br, —$CH_2C\mathbf{H_2}C(O)O$—, 2H), 3.47 (br, —NC$\mathbf{H_2}$—, 2H), 4.66 (m, $^2J_{H\text{-}H}$ = 34.6 Hz, $^3J_{H\text{-}F}$ = 12.1 Hz, —$CF(CF_3)C\mathbf{H_2}O$—, 2H), 6.63 (s, —C**H**═C**H**—, 2H) ^{13}C NMR (101 MHz, C_6D_6, δ): 22.4 (—$NCH_2\mathbf{C}H_2CH_2$—), 30.2 (—$CH_2\mathbf{C}H_2C(O)O$—), 36.4 (—N**C**H_2—), 59.4 (d, $^2J_{C\text{-}F}$ = 31.4 Hz, —$CF(CF_3)\mathbf{C}H_2O$—), 134.0 (—**C**H═**C**H—), 170.7 (—(**C**O)—CH═CH—(**C**O)—), 170.8 (—$CF(CF_3)CH_2O(\mathbf{C}O)$—) ^{19}F NMR (376 MHz, C_6D_6, δ): −134.3 $R_fC\mathbf{F_2}(CF_3)CH_2O(CO)R_h$ GC–MS, 70 eV, *m/z*: 69.1 (37), 82.1 (15), 100 (14), 110.1 (51), 119 (13), 124.1 (14), 137.1 (16), 138.1 (23), 147 (24), 150 (28), 165.1 (18), 166.1 (76), 169 (100), 335 (18), 528.2 (14) MALDI-TOF, $[M + Li]^+$: 1818.6–1984.8–2151.0–2316.3–2482.5 FTIR (ATR) ν_{max} (cm^{-1}): 828.0–982.4–1126.3–1232.4–1715.7.

M2 C5 **4b** (yield = 84%): ^{1}H NMR (400 MHz, C_6D_6, δ): 1.28 (br, —N$(CH_2)_2(C\mathbf{H_2})CH_2$—, 2H), 1.54 (br, —$NCH_2C\mathbf{H_2}$—, 2H), 1.62 (br, N$(CH_2)_8C\mathbf{H_2}CH_2C(O)O$—, 2H), 2.34 (br, —$CH_2C\mathbf{H_2}C(O)O$—, 2H), 3.43 (br, —NC$\mathbf{H_2}$—, 2H), 4.69 (m, $^2J_{H\text{-}H}$ = 31.4 Hz, $^3J_{H\text{-}F}$ = 12.8 Hz, —$CF(CF_3)C\mathbf{H_2}O$—, 2H), 6.67 (s, —C(O)C**H**═C**H**C(O)—, 2H) ^{13}C NMR (101 MHz, C_6D_6, δ): 23.9 $(NCH_2(CH_2)_2\mathbf{C}H_2CH_2C(O)O$—), 25.9 (—$NCH_2\mathbf{C}H_2$—), 28.0 (—$N(CH_2)_2(\mathbf{C}H_2)CH_2$—), 32.8 (—$CH_2\mathbf{C}H_2C(O)O$—), 37.1 (—N**C**$H_2$—), 59.2 (d, $^2J_{C\text{-}F}$ = 30.4 Hz, —$CF(CF_3)\mathbf{C}H_2O$—), 134.0 (—**C**H═**C**H—), 170.6 (—(**C**O)—CH═CH—(**C**O)—), 171.1 (—$CF(CF_3)CH_2O(\mathbf{C}O)$—) ^{19}F NMR (376 MHz, C_6D_6, δ): −134.9 $R_fC\mathbf{F_2}(CF_3)CH_2O(CO)R_h$ GC–MS, 70 eV, *m/z*: 54 (10), 55 (12), 69.2 (37), 82.2 (15), 100 (21), 110 (100), 111 (16), 147 (16), 150 (31), 169 (88), 193.1 (15), 194.1 (32), 335.1 (16) MALDI-TOF, $[M + Li]^+$: 1846.6–2012.8–2179.1–2344.3–2510.5 FTIR (ATR) ν_{max} (cm^{-1}): 827.0–978.9–1117.4–1226.9–1711.6.

M2 C10 **4c** (yield = 86%): ^{1}H NMR (400 MHz, C_6D_6, 50 °C, δ): 1.22 (m, —$N(CH_2)_2(C\mathbf{H_2})_6CH_2$—, 12H), 1.49 (br, —$NCH_2C\mathbf{H_2}$—, 2H), 1.56 (br, $N(CH_2)_8C\mathbf{H_2}CH_2C(O)O$—, 2H), 2.29 (br, —$CH_2C\mathbf{H_2}C(O)O$—, 2H), 3.39 (br, —NC$\mathbf{H_2}$—, 2H), 4.60 (m, $^2J_{H\text{-}H}$ = 34.6 Hz, $^3J_{H\text{-}F}$ = 12.3 Hz, —$CF(CF_3)C\mathbf{H_2}O$—, 2H), 6.61 (s, —C**H**═C**H**—, 2H) ^{13}C NMR (100 MHz, C_6D_6, δ): 24.5 (—$\mathbf{C}H_2CH_2C(O)O$—), 26.9 (—$NCH_2\mathbf{C}H_2$—), 28.7–29.6 (—$N(CH_2)_2(\mathbf{C}H_2)_6CH_2$—), 33.0 (—$CH_2\mathbf{C}H_2COO$—), 37.6 (—N**C**$H_2$—), 59.2 (d, $^2J_{C\text{-}F}$ = 30.5 Hz, —$CF(CF_3)\mathbf{C}H_2O$—), 134.2 (—**C**H═**C**H—), 170.7 (—(**C**O)—CH═CH—(**C**O)—), 171.0 (—$CF(CF_3)CH_2O(\mathbf{C}O)$—) ^{19}F NMR (376 MHz, C_6D_6, δ): −135.0 $R_fC\mathbf{F_2}(CF_3)CH_2O(CO)R_h$ GC–MS, 70 eV, *m/z*: 54.9 (11), 69 (53), 82 (24), 83.1 (12), 100 (26), 110 (100), 111 (16), 119 (16), 147 (16), 150.1 (32), 169.1 (87), 191.1 (14), 263.1 (30), 264.3 (46), 335 (19) MALDI-TOF, $[M + Li]^+$: 1917.0–2083.2–2249.5–2414.7–2581.0 FTIR (ATR) ν_{max} (cm^{-1}): 826.9–979.1–1117.6–1227.1–1710.6.

RESULTS AND DISCUSSION

Synthesis of the Maleimide PFPAEs

Five different maleimides were synthesized according to Scheme 2 and their structures are depicted in Figure 1: they are characterized by PFPAE chains of different lengths (*n* = 6.5 for M_x = M1 and *n* = 11 for M_x = M2) and by a different spacer of 3, 5, 10-methylene units (—CH_2— unit) between the fluorinated chain and the maleimide group. The products will be named M_x C3, M_x C5, M_x C10, respectively.

The starting materials employed are two different oligo (HFPO) methylene alcohols M_x having a molecular weights of 1250 g/mol (*n* = 6.5) and 2000 g/mol (*n* = 11) labeled M1 and M2, respectively. The shortest molecular weight (i.e. 1250 g/mol) comes from the reduction of Krytox® acyl fluoride from Chemours Company whereas the longer molecular weight Krytox® methylene alcohol (i.e. 2000 g/mol) was directly provided by Chemours Company.

In this work, the synthesis of PFPAEs maleimides was performed via a two-step or three-step reaction. The maleimides which were used were either commercial products (**1c**) or synthesized maleimides (**1a-b**) (see Experimental section). Two different esterification methods were then used.

Macromonomers **3b-c** were efficiently synthesized via nucleophilic acyl substitution of the oligo(HFPO) alcohol M1 with

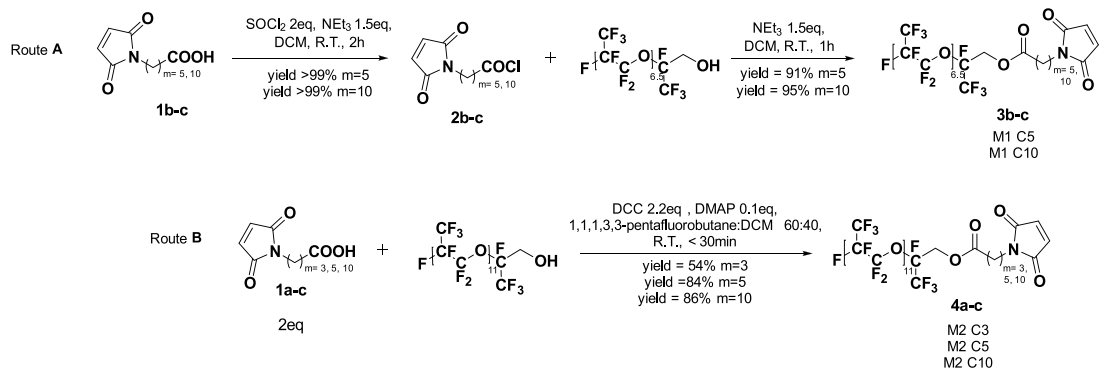

SCHEME 2 Reaction scheme of the addition of maleimide groups to fluorinated oligomers.

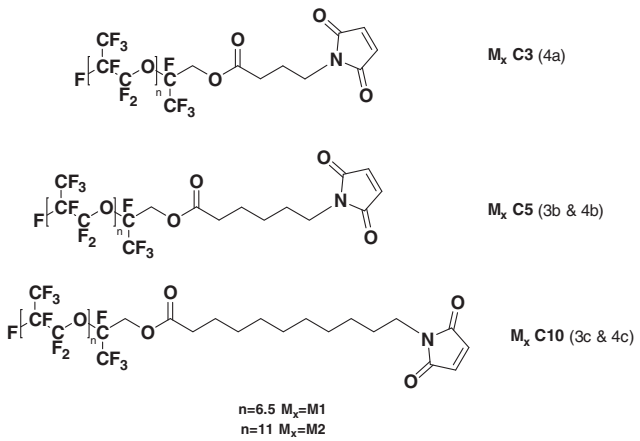

FIGURE 1 Structures of the different maleimide PFPAEs.

the corresponding acyl chlorides (**2b-c**; the chlorinated analogues of **1b-c**) (Scheme 2, Route A). However, **4a-c** (containing the longer fluorinated chains) did not reach complete conversion by Route A. Previous work has shown Steglich esterification to provide a facile route for oligo (HFPO) methylene alcohol esterification, and this method enabled the successful synthesis of **4a-c** (Route B).[35]

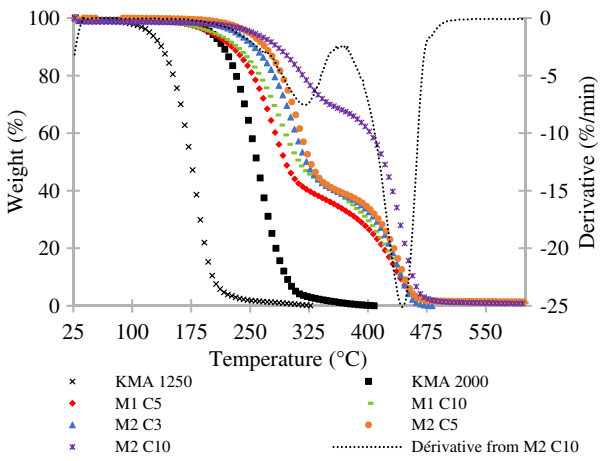

FIGURE 2 TGA curves of the starting Krytox® Methylene Alcohol (KMA) and the monomers M1 C5, M1 C10, M2 C3, M2 C5, and M2 C10 under nitrogen. [Color figure can be viewed at wileyonlinelibrary.com]

According to thermal analysis, the maleimide functionalized PFPAE macromonomers exhibited improved thermal stability over the corresponding starting PFPAE alcohol. For example, Krytox® methylene alcohol M_w ~ 1250 g/mol had a $T_{5\%}$ of 122 °C. With the substituents C5 and C10 added to the methylene alcohol, the $T_{5\%}$ was increased up to 200 °C for both products. For Krytox® methylene alcohol M_w ~ 2000 g/mol, the $T_{5\%}$ was increased from 200 °C for the starting alcohol to 233, 248, and 253 °C for M2 C3, M2 C5, and M2 C10 respectively. However, the maleimide was expected to polymerize before complete degradation explaining the two different steps by thermogravimetric analyses (TGA). The derivative highlights the presence of two distinct peaks which means two steps of degradation (Fig. 2).

In order to determine the phenomena that gave rise to these two degradation peaks, thermogravimetric analysis coupled with infrared spectroscopy was used to identify the degradation products. The information provided by Figure 3 is the disappearance of the maleimide C═C bond (sp^2 C—H bending) at 826 cm^{-1} during the second degradation step. Thus, it implies that the first degradation pathway was the loss of the monomer with the presence of a band at 826 cm^{-1}. Next, the heat transfer from the TGA causes additional polymerization of the maleimide with no substantial weight loss, and finally the second degradation is evident as the maleimide polymer deteriorates.

Kinetics Studies of Maleimide PFPAEs

The new maleimides were used as reactive monomers in photopolymerization. Photopolymerization kinetics were monitored by Real Time-FTIR. The effect of structural parameters was first studied and discussed depending on their photopolymerization kinetics. Then the photopolymerization conditions such as the presence of air and photoinitiator will be discussed.

Influence of the Molecular Weight of the PFPAE Chain (M1-M2)

For the same hydrogenated spacer C5, two different products with two PFPAE chains were tested: M1 C5 and M2 C5. The

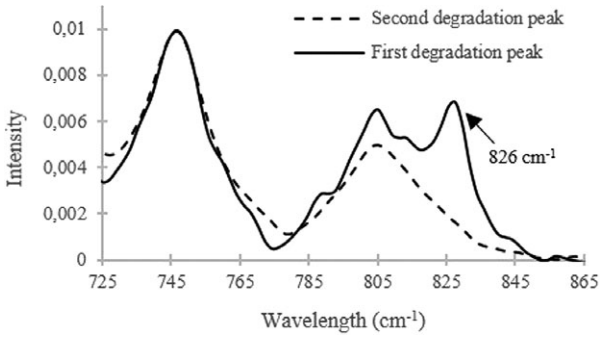

FIGURE 3 IR spectra of the degradation products during the first and second degradation steps.

conversion over time was calculated by measuring the decrease of the C═C band (sp^2 C—H bending) at 826 cm^{-1} until quantitative conversion of the products were evident. At 696 cm^{-1}, the C═C band loss also confirmed its complete disappearance (see Supporting Information). The higher molecular weight monomer (M2 C5) reached quantitative conversion in 10 s, while the lower molecular weight monomer (M1 C5) reached only 17% conversion in the same period of time (Fig. 4). Longer UV-curing time was required for M1 C5 to get to quantitative conversion (70 s). The assumption for the faster conversion rates is due to the higher percentage of fluorine. As fluorine content increases, there is larger amount of submicron segregation between the hydrogenated and fluorinated chains. Thus it promotes the increased probability of hydrogenated segments encountering each other for polymerization.

Influence of the Hydrogenated Spacer and Air on Maleimide Oligo(HFPO) M1

When the homopolymerization of the maleimide monomers M1 C5 and M1 C10 were performed in the absence of air as shown on Figure 5, both monomers achieved quantitative conversion by 70 s. They both reached roughly 95% conversion in 40 s. However, M1 C10 exhibited a greater initial rate of polymerization than M1 C5, which could be due to the increased flexibility of the longer hydrogenated spacer C10. A higher flexibility could help to facilitate the submicron segregation and then increase the proximity of the hydrogenated maleimides.

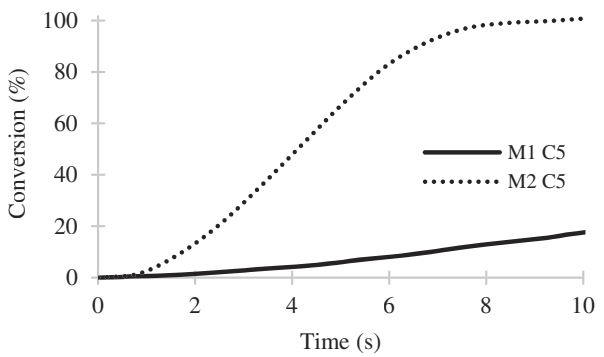

FIGURE 4 Photopolymerization conversion curves of M1 C5 and M2 C5 without air.

Maleimides are known to demonstrate less oxygen inhibition than (meth)acrylate systems.[36] Indeed, both monomers, M1 C5 and M1 C10, achieved complete conversion in the absence and in the presence of air (Fig. 5). However, oxygen inhibition was observed. M1 C5 demonstrated a higher oxygen inhibition as a complete conversion was obtained after more than 400 s under air. On the contrary, M1 C10 showed a complete conversion in less than 150 s under air. Consequently, the difference between both hydrogenated spacers C5 and C10 was more visible in the presence of air. Moreover, it is notable that oxygen has greater solubility in organic solvents with longer aliphatic chains (e.g., heptane and octane), and lower solubility in those with shorter aliphatic chains (e.g., pentane and hexane).[37] Therefore, the decreased oxygen solubility afforded by the longer hydrogenated spacer in M1 C10 monomer could explain this monomer's greater resistance to oxygen inhibition and increased reaction rate compared to M1 C5.

Influence of the Hydrogenated Spacer and Air on Maleimide Oligo (HFPO) M2

In comparison to the lower molecular weight (M1 products), the hydrogenated spacer was not a key factor for the reaction speed for M2 products due to the longer HFPO segment. Complete conversion was reached after 8 s without air and after 40 s in the presence of air (Fig. 6). Oxygen inhibition was observed at the beginning until 10 s and then the reaction speed increased (Fig. 6). Nonetheless, all M2 products reached quantitative conversion at the same time in comparison to M1 products.

Influence of the Presence of Photoinitiator

As mentioned earlier, maleimides can polymerize without photoinitiators. However, it seems interesting to evaluate the effect of the photoinitiator on the photopolymerization processes without air and M2 C10 was chosen as the reference. Three different Norrish II-type photoinitiators were used: BAPO, TPO, and 2-hydroxy-2-methylpropiophenone (Darocur 1173). The photoinitiator efficiency follows this order: TPO > BAPO > Darocur (Fig. 7). Only TPO permitted faster photopolymerization kinetics than the maleimide on its own (Table 1). Having a photoinitiator seemed to increase the reaction speed during the first seconds but after 80%–90% of conversion, the reaction speed slowed down. Therefore, the conversion rates seemed to differ between the reactions with and without photoinitiators. However, in 15 s, a quantitative conversion was obtained for the pure M2 C10, TPO, and BAPO. Darocur 1173 showed the lowest solubility by forming a gel with M2 C10 which could explain the slower conversion.

A cut-off filter was also employed (irradiation area: 400–500 nm) for some experiments to avoid absorption of light by the maleimide[36] and to induce initiation exclusively by the photoinitiator. The aim of the filter was to separate the initiating and the propagation steps. Two initiators were effective in this zone: BAPO and TPO due to an absorption between 400 and

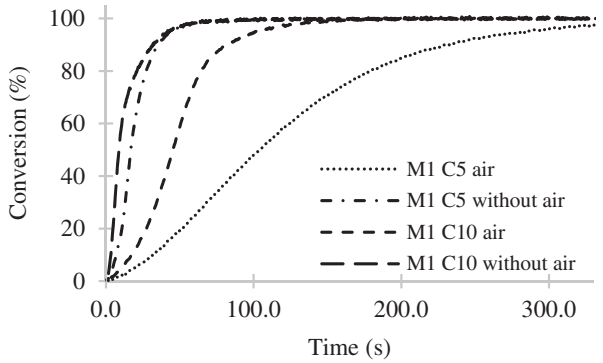

FIGURE 5 Photopolymerization conversion curves for M1 C5 and M1 C10 with and without air.

500 nm. However, Darocur 1173 does not absorb in this zone. Consequently, in the presence of a filter, no conversion was noted for the pure product as well as in the presence of Darocur 1173 (Table 1). Nonetheless, TPO showed a faster conversion than BAPO. Moreover, in the presence of a filter, an inhibition step was detected at the beginning. Therefore, the initiating step appeared to last 1.5 and 2 s for TPO and BAPO, respectively, and then the reactions went until complete conversion in 17 s for TPO and in 50 s for BAPO (Table 1). In any case, the use of photoinitiator was not essential as the difference between no photoinitiator and TPO is very slight to reach the quantitative conversion: 8 versus 5 s in the absence of photoinitiator.

Thermal and Surface Properties

The starting monomers as well as the cured polymers were analyzed by TGA and DSC. Contact angle measurements were also performed by using distilled water and hexadecane.

Thermogravimetric Analyses

The different maleimides were tested by TGA to study their thermal behavior.

The homopolymers M1 C5 and M1 C10 exhibited a T5% of 230 °C and 277 °C respectively. The difference in hydrocarbon chain lengths clearly showed an improvement for the T5%.

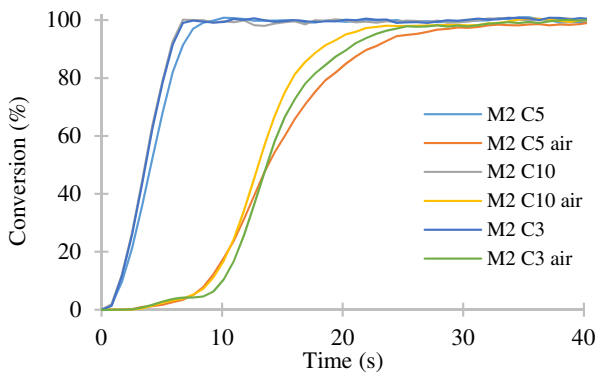

FIGURE 6 Photopolymerization conversion curves for M2 C3, C5, and C10 with and without of air. [Color figure can be viewed at wileyonlinelibrary.com]

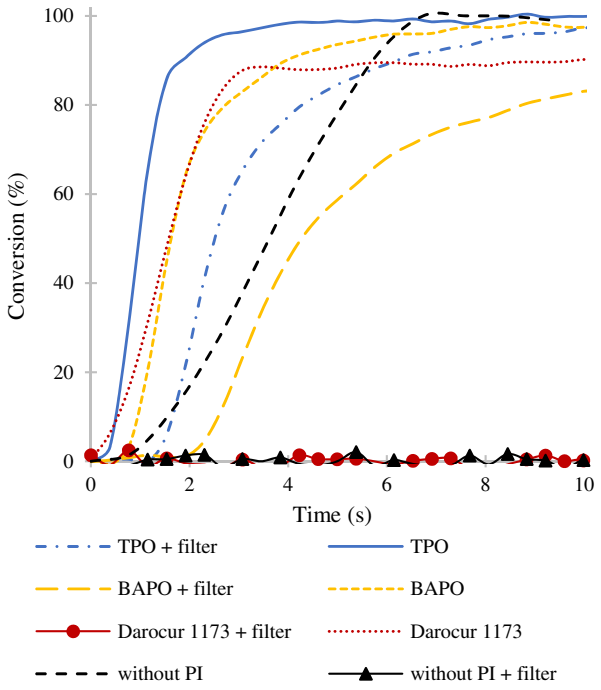

FIGURE 7 Photopolymerization curves for the use of different photoinitiators (2% w/w) and a cut-off filter. [Color figure can be viewed at wileyonlinelibrary.com]

For the highest molecular weight oligo(HFPO) M2 series, the T5% temperatures were 306 °C, 323 °C and 336 °C for M2 C3, M2 C5 and M2 C10 respectively. The longer the spacer the higher the T5% as for M1 polymers. All displayed better thermal stability than their corresponding monomers (Fig. 8).

These degradation temperatures demonstrate a good thermal resistance in comparison to a previous study about the copolymers (maleate-*alt*-vinyl ether) PFPAEs.[35] The most thermally stable homopolymer M2 C10 ($T_{10\%}$ - 10 K/min: 360 °C in N_2 and 292 °C in air—Figure 9) showed higher thermal stability than crosslinked PFPAEs with acrylate bonds ($T_{10\%}$ - N_2 = 256–280 °C).[38] They were also comparable to materials

TABLE 1 Table of the Experimental Conditions With and Without Photoinitiators (2% w/w)

Sample	Inhibition Delay (s)	Quantitative Conversion Time (s)	Conversion Rate at 10 s (%)
Without PI	>1	8	100
Without PI + filter	–	No conversion	0
TPO	>0.5	5	100
TPO + filter	1.5	17	97
BAPO	>1	15	97.5
BAPO + filter	2	50	83
Darocur 1173	0	130	90
Darocur 1173 + filter	–	No conversion	0

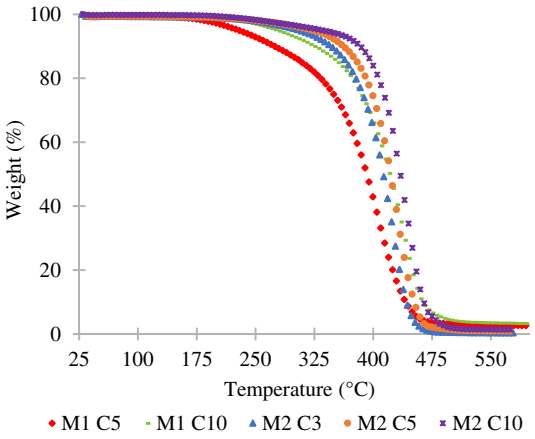

FIGURE 8 TGA curves of polymers after UV-curing under nitrogen. [Color figure can be viewed at wileyonlinelibrary.com]

based on stronger triazole bonds under air ($T_{10\%}$ = 305 and 336 °C) containing PFPAEs and perfluoroalkyl chains.[39] However, the maleimides obviously showed a faster degradation kinetic in presence of air and seemed to be more sensitive to oxidation degradation even if these non-crosslinked polymers provided good results in terms of thermal stability.

DSC Analyses

The glass transition temperatures of the different homopolymers were also studied. They displayed very similar values from −71 to −66 °C for the homopolymers. In any case, only the glass transition temperatures of the fluorinated phase were detected. Indeed, as it is a branched homopolymer containing many fluorinated units for each maleimide unit, it overlapped the effect of the hydrogenated counterpart from the maleimide groups. Another observation concerns the $T_{melting}$ for only one of the experimental monomers, M2 C10. The melting point ($T_{melting}$) for this monomer was −23 °C. This is due to the long aliphatic chain of C10 and has a comparable melting point to decane, $T_{melting}$ = −29.7 °C. However, surprisingly, no melting temperature was observed for M1 C10 (see Supporting Information).

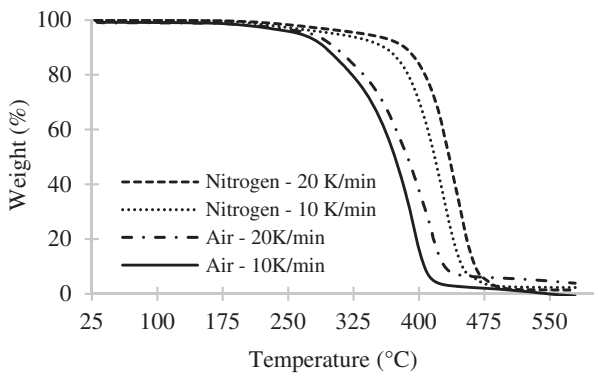

FIGURE 9 TGA curves of UV-cured M2C10 under nitrogen and air at different heating rates.

TABLE 2 Contact Angle Values for Water and Hexadecane

Contact Angle (°)	M1 C5	M1 C10	M2 C3	M2 C5	M2 C10
Water	113	117	99	104	124
Hexadecane	76	78	66	67	82

Contact Angle Measurements

After spin-coating the maleimide PFPAEs onto glass slides and photopolymerizing them using a conveyor bench, the contact angles of the products were examined.

The polymers revealed hydrophobic and oleophobic properties (Table 2). In this study, the contact angles were dependent on the chain flexibility afforded by the hydrogenated spacer. The longer the spacer the better flexibility and consequently, the better segregation permitted. These attributes lead to higher contact angle values. It was assumed that the segregation occurred due to the glass support and altered the contact angles. It has already been reported for crosslinked methacrylate PFPAEs with different contact angles between the air and the glass sides.[40,41] Moreover, the values are in good agreement with previous values found for methacrylate PFPAEs homopolymers[42] or crosslinked acrylates PFPAEs.[38,43] By using hexadecane, the same trend was observed: an increase of the hydrogenated spacer length permitted an increase in contact angle values. The omniphobic properties were then proved and the polymers can be used for water–oil repellent applications.

CONCLUSIONS

Maleimide groups bonded to PFPAEs allowed for very rapid polymerization under UV-light without photoinitiator. The effect of molecular weight of the oligo(HFPO) was most significant. Longer fluorinated chains permitted increased segregation of the hydrocarbon and fluorocarbon portions of the polymer. This higher degree of segregation increased the rate of polymerization. Moreover, the effect of the hydrogenated spacer was then hidden by the highest molecular weight HFPO chain. The presence of air showed a slight influence in comparison to some acrylic systems. Indeed, even if oxygen inhibition was observed at the beginning, complete conversion was easily obtained. These homopolymers also exhibited excellent thermal and omniphobic properties that are far superior to those of crosslinked acrylate PFPAE materials previously used in microfluidics.

ACKNOWLEDGMENTS

This research project has received funding from the European Union's Horizon 2020 Marie Skłodowska-Curie Actions program under Grant Agreement No. 690917 – PhotoFluo; Natural Sciences and Engineering Research Council of Canada (NSERC), Discovery Grants Program RGPIN-2015-05513, and Ministère de l'Enseignement Supérieure et de la Recherche.

REFERENCES AND NOTES

1 G. Oster, N. L. Yang, *Chem. Rev.* **1968**, *68*(2), 125.

2 J. V. Crivello, E. Reichmanis, *Chem. Mater.* **2014**, *26*(1), 533.

3 C. E. Hoyle, C. N. Bowman, *Angew. Chem. Int. Ed.* **2010**, *49*(9), 1540.

4 Y. Du, B. A. Williams, L. F. Francis, A. V. McCormick, *Prog. Org. Coat.* **2017**, *104*, 104.

5 Y. Du, J. Xu, J. D. Sakizadeh, D. G. Weiblen, A. V. McCormick, L. F. Francis, *ACS Appl. Mater. Interfaces* **2017**, *9*(29), 24976.

6 J. von Sonntag, D. Beckert, W. Knolle, R. Mehnert, *Radiat. Phys. Chem.* **1999**, *55*(5–6), 609.

7 J. von Sonntag, W. Knolle, *J. Photochem. Photobiol. A: Chem.* **2000**, *136*(1–2), 133.

8 C. P. Vázquez, C. Joly-Duhamel, B. Boutevin, *Macromol. Chem. Phys.* **2009**, *210*(3–4), 269.

9 C. E. Hoyle, S. C. Clark, S. Jonsson, M. Shimose, *Polymer* **1997**, *38*(22), 5695.

10 S. Jönsson, P. E. Sundell, M. Shimose, S. Clark, C. Miller, F. Morel, C. Decker, C. E. Hoyle, *Nucl. Instrum. Methods Phys. Res., Sect. B* **1997**, *131*(1–4), 276.

11 C. Pozos Vázquez, R. Tayouo, C. Joly-Duhamel, B. Boutevin, *J. Polym. Sci., Part A: Polym. Chem.* **2010**, *48*(10), 2123.

12 K.-D. Ahn, J.-H. Kang, K. W. Yoo, D. J. Choo, *Macromol. Symp.* **2007**, *254*(1), 46.

13 E. Dolci, V. Froidevaux, C. Joly-Duhamel, R. Auvergne, B. Boutevin, S. Caillol, *Polym. Rev.* **2016**, *56*(3), 512.

14 J. M. Barrales-Rienda, J. G. Ramos, M. S. Chavez, *J. Fluorine Chem.* **1977**, *9*(4), 293.

15 J. M. Barrales-Rienda, J. G. Ramos, M. S. Chaves, *J. Polym. Sci. Polym. Chem. Ed.* **1979**, *17*(1), 81.

16 S. M. Mokhtar, S. M. Abd-Elaziz, F. A. Gomaa, *J. Fluorine Chem.* **2010**, *131*(5), 616.

17 P. Hendlinger, A. Laschewsky, P. Bertrand, A. Delcorte, R. Legras, B. Nysten, D. Möbius, *Langmuir* **1997**, *13*(2), 310.

18 D. Jain, J. Maheshwari, N. Rathore, S. N. Paliwal, J. Rasayan, *Chemistry* **2012**, *5*(4), 445.

19 L. Daukiya, C. Mattioli, D. Aubel, S. Hajjar-Garreau, F. Vonau, E. Denys, G. Reiter, J. Fransson, E. Perrin, M. L. Bocquet, C. Bena, A. Gourdon, L. Simon, *ACS Nano* **2017**, *11*(1), 627.

20 O. Beaune, J. M. Bessière, B. Boutevin, J. J. Robin, *J. Fluorine Chem.* **1994**, *67*(2), 159.

21 B. Boutevin, J. M. Lusinchi, Y. Pietrasanta, J. J. Robin, *J. Fluorine Chem.* **1995**, *73*(1), 79.

22 A. Soules, C. Pozos Vázquez, B. Améduri, C. Joly-Duhamel, M. Essahli, B. Boutevin, *J. Polym. Sci., Part A: Polym. Chem.* **2008**, *46*(10), 3214.

23 W. Cummings, E. R. Lynch, Polyimides, Patent GB1077243A, **1965**.

24 H. E. Green, R. J. Jones, M. K. O'Rell, Bis di(fluoromaleimide) capped polymers, U.S. Patent 4,173,700, **1989**.

25 C.-Y. Shiue, A. P. Wolf, J. F. Hainfeld, *J. Labelled Compd. Radiopharm.* **1989**, *26*(1–12), 287.

26 B. De Bruin, B. Kuhnast, F. Hinnen, L. Yaouancq, M. Amessou, L. Johannes, A. Samson, R. Boisgard, B. Tavitian, F. Dollé, *Bioconjug. Chem.* **2005**, *16*(2), 406.

27 Y. Fujita, Y. Murakami, A. Noda, S. Miyoshi, *Bioconjug. Chem.* **2017**, *28*(2), 642.

28 M. Berndt, J. Pietzsch, F. Wuest, *Nucl. Med. Biol.* **2007**, *34*(1), 5.

29 F. Dollé, F. Hinnen, B. Lagnel, R. Boisgard, A. Sanson, F. Russo-Marie, B. Tavitian, *J. Labelled Compd. Radiopharm.* **2003**, *46*(S1), S15.

30 W. Cai, X. Zhang, Y. Wu, X. Chen, *J. Nucl. Med.* **2006**, *47*(7), 1172.

31 B. Ameduri, B. Boutevin, *Well-Architectured Fluoropolymers: Synthesis, Properties and Applications*, Elsevier B.V: Amsterdam, **2004**, p. 187.

32 G. Malinverno, G. Pantini, J. Bootman, *Food Chem. Toxicol.* **1996**, *34*(7), 639.

33 G. Pantini, *Clin. Dermatol.* **2008**, *26*(4), 387.

34 C. Zhang, S. S. Moonshi, W. Wang, H. T. Ta, Y. Han, F. Y. Han, H. Peng, P. Král, B. E. Rolfe, J. J. Gooding, K. Gaus, A. K. Whittaker, *ACS Nano* **2018**, *12*(9), 9162.

35 C. Bonneaud, M. Decostanzi, J. Burgess, G. Trusiano, T. Burgess, R. Bongiovanni, C. Joly-Duhamel, C. M. Friesen, *RSC Adv.* **2018**, *8*(57), 32664.

36 C. Decker, C. Bianchi, F. Morel, S. Jönsson, C. Hoyle, *Macromol. Chem. Phys.* **2000**, *201*(13), 1493.

37 T. Sato, Y. Hamada, M. Sumikawa, S. Araki, H. Yamamoto, *Ind. Eng. Chem. Res.* **2014**, *53*(49), 19331.

38 R. Bongiovanni, A. Medici, A. Zompatori, S. Garavaglia, C. Tonelli, *Polym. Int.* **2012**, *61*(1), 65.

39 G. Lopez, B. Ameduri, J. P. Habas, *Macromol. Rapid Commun.* **2016**, *37*(8), 711.

40 Z. Hu, L. Chen, D. E. Betts, A. Pandya, M. A. Hillmyer, J. M. DeSimone, *J. Am. Chem. Soc.* **2008**, *130*(43), 14244.

41 Y. Wang, L. M. Pitet, J. A. Finlay, L. H. Brewer, G. Cone, D. E. Betts, M. E. Callow, J. A. Callow, D. E. Wendt, M. A. Hillmyer, J. M. DeSimone, *Biofouling* **2011**, *27*(10), 1139.

42 R. Bongiovanni, A. Di Meo, A. Pollicino, A. Priola, C. Tonelli, *React. Funct. Polym.* **2008**, *68*(1), 189.

43 A. Vitale, A. Priola, C. Tonelli, R. Bongiovanni, *Polym. Int.* **2013**, *62*(9), 1395.